EUROPHYSICS LETTERS 1 August 2001

Europhys. Lett., **55** (3), pp. 303–309 (2001)

On the classical limit in atom-surface diffraction

A. S. Sanz[1], F. Borondo[1] and S. Miret-Artés[2]

[1] *Departamento de Química, C-IX, Universidad Autónoma de Madrid Cantoblanco, 28049 Madrid, Spain*

[2] *Instituto de Matemáticas y Física Fundamental, CSIC Serrano 123, 28006 Madrid, Spain*

(received 5 April 2001; accepted 21 May 2001)

PACS. 03.65.-w – Quantum mechanics.
PACS. 03.65.Ta – Foundations of quantum mechanics; measurement theory.
PACS. 79.20.Rf – Atomic, molecular and ion beam impact and interactions with surfaces.

Abstract. – The transition to the classical limit in atom-surface diffraction is studied using the de Broglie-Bohm causal formalism. In particular, we focus on rainbow scattering, which is a well-defined effect in classical mechanics and has a clear counterpart in quantum mechanics. In order to achieve this limit, we consider the scattering of particles with increasing masses off a Cu(110) surface. Although the classical limit seems strictly unreachable, quantum trajectories mimic the characteristics of the classical intensity distribution, and their use allows to unveil the mechanism by which the quantum rainbow condition takes place.

Diffraction of atoms (specially rare gases) and small diatomic molecules off solid surfaces is presently a very active field of research [1]. Typical diffracting systems consist of single-metal surfaces and transmission gratings [2]. The corresponding experiments lead to a better knowledge of the ubiquitous van der Waals interactions, surface characterization and, in general, to the improvement of atomic optics and atom interferometry [3]. In particular, by increasing the mass of the impinging particles, higher angular and energy resolutions are necessary to detect a larger number of weak and sharp diffraction peaks. In the interpretation of these scattering experiments with heavy projectiles classical mechanics is frequently used, a procedure that must be exerted with caution since the semiclassical limit is highly non-uniform [4]. Moreover, there are recent experiments in which the quantum behavior of such particles has been observed [5].

The purpose of this letter is to provide a pure quantum explanation of this kind of phenomena within the causal point of view of the de Broglie-Bohm (BB) quantum theory of motion [6, 7]. In our opinion, this theory has the important additional advantage of opening up new perspectives into the long-standing and open problem of the correspondence between quantum and classical mechanics [8, 9]. To achieve this goal, we have selected to study the rainbow effect, for which there is a clear and unique correspondence between quantum and classical features, considering the latter as a limiting case of the former.

In the last years there has been a renewed interest in the BB theory as a framework to provide intuitive insight into quantum problems, in particular, quantum interference and diffraction. This theory has been successfully applied to a great variety of problems [10].

Very recently, atom diffraction by metal surfaces has been studied by the authors using this theory [9]. In that work, concepts like the Fresnel and Fraunhofer regimes of undulatory optics or the classical turning points defining the surface electronic density have been revisited from a full quantum perspective.

The fundamental equations in the BB theory [7] are derived by introducing the wave function $\Psi(\boldsymbol{r},t) = R(\boldsymbol{r},t)\, e^{iS(\boldsymbol{r},t)/\hbar}$ (R and S are real valued) into the time-dependent Schrödinger equation to obtain

$$\frac{\partial R^2}{\partial t} + \nabla\left(\frac{R^2 \nabla S}{m}\right) = 0\,, \tag{1}$$

$$\frac{\partial S}{\partial t} + \frac{(\nabla S)^2}{2m} + V + Q = 0\,, \tag{2}$$

which are the continuity and quantum Hamilton-Jacobi equations, respectively; here m is the mass of the incoming particle, and V the gas-surface interaction. The last term in eq. (2) is the so-called quantum potential, defined as

$$Q = -\frac{\hbar^2}{2m}\frac{\nabla^2 R(\boldsymbol{r},t)}{R(\boldsymbol{r},t)}\,. \tag{3}$$

This potential is determined by the quantum state of the system, and together with V determines the acting forces. Within this formulation the correspondence principle is mathematically expressed as $Q \to 0$. In our case, this limit will be achieved by increasing the value of m.

Quantum trajectories are calculated by integrating the particle equation of motion, $\dot{\boldsymbol{r}} = \nabla S(\boldsymbol{r},t)/m$, similarly to what happens in the classical Hamilton-Jacobi theory [11]. According to the statistical interpretation of quantum mechanics, these trajectories are paths along which probability flows, and therefore they are directly related to the probability current as well.

As a working example, we have chosen the He-Cu(11α) surface collisions, which have been extensively studied in the past, both experimentally [12,13], and theoretically at quantum [14], semiclassical [15] and classical [16] level. In particular we consider the quasi–one-dimensional and least corrugated face, Cu(110), for which the out-of-plane collisions are negligible, and thus a 2D Hamiltonian model can be used,

$$H = (p_x^2 + p_z^2)/2m + V(x,z), \tag{4}$$

where x and z are the directions parallel and perpendicular to the surface, respectively. The interaction potential is described by a corrugated Morse function

$$V(x,z) = D\, e^{-2\alpha z}\,[1 - 2e^{\alpha z} + (0.03\cos 2\pi x/a + 0.0004\cos 4\pi x/a)], \tag{5}$$

where the Morse parameters ($\alpha = 1.05$ Å^{-1} and $D = 6.35$ meV) and the unit cell length ($a = 3.6$ Å) have been taken from the literature [12].

In order to describe the transition to the classical limit, we have considered increasingly larger values for m, taking the rare-gas sequence: He, Ne, Ar, and finishing with a fictitious particle, labelled He*, with $m_{\mathrm{He}^*} = 500\ m_{\mathrm{He}}$, maintaining the same potential. Notice that this way to proceed implies some approximations. In the first place, the attractive potential depths, as well as the surface corrugation amplitudes and inelastic contributions, are expected to be larger as the mass of the incident particle increases. Second, although the wave character is not negligible for heavy rare gases, no well-resolved in-plane diffraction peaks and out-of-plane diffraction intensities have been observed experimentally, specially for Ar [13]. However, rainbow features have been identified for Ne and Ar, which display no shift with

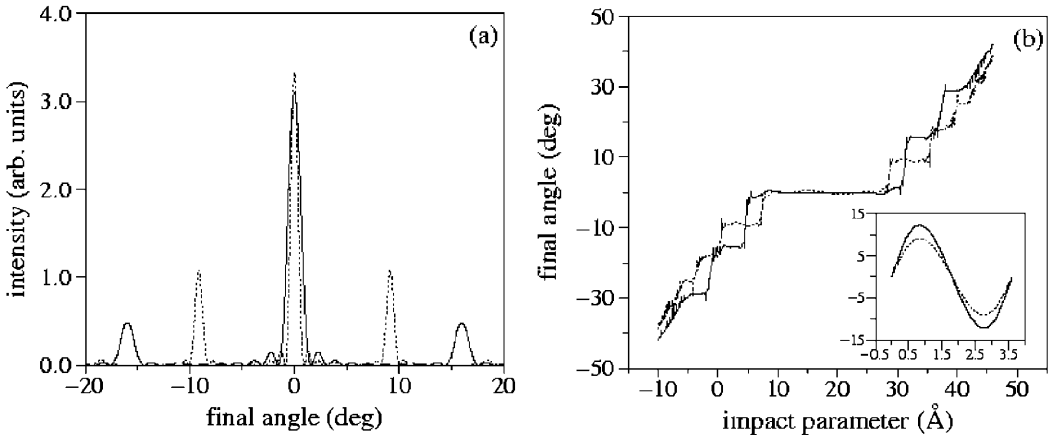

Fig. 1 – Intensity diffraction pattern (a) and quantum deflection function (b) for the He-Cu(110) scattering at 21 meV (solid line) and 63 meV (dotted line) and normal incidence. The corresponding classical deflection functions are also plotted in the inset to panel (b).

the surface temperature. To minimize the impact of all those effects in our final conclusions, the calculations have been performed at normal incidence, $\theta_i = 0°$, and with incident energies compared to the potential well.

From the classical point of view, the rainbow singularity is explained by the presence of caustics [17], where the corresponding semiclassical wave function breaks down. Quantum mechanically, this singularity is usually replaced by an intensity maximum in the angular distribution, and the quantum rainbow condition takes place when the classical raibow coincides with a Bragg channel. In this respect, it has been argued that rainbow features should be associated to the whole diffraction pattern instead of a very high-intensity diffraction peak, which does not necessarily correspond to the diffraction channel displaying rainbow [15]. As will be shown later, by comparing quantum (within the BB theory) and classical trajectories deflection angle distributions, this intuitive interpretation is well justified.

The numerical procedure used in this work has been described in detail in ref. [9]. It starts by simultaneously propagating the initial wave packet, according to the method proposed by Heller [18], and running quantum trajectories. After these trajectories have been computed, the quantum deflection (QD) function, *i.e.*, the distribution of final scattering angles *vs.* the impact parameter, defined as the initial position over the surface at which trajectories are started, is evaluated.

In fig. 1 the results for the scattering of He atoms at two values of the total energy, $E_i = 21$ and 63 meV, are plotted in solid and dotted lines, respectively. Part (a) corresponds to the diffraction pattern calculated using the S-matrix method of ref. [18], while in panel (b) the corresponding QD function is given. We also present, in the inset, the corresponding classical deflection (CD) functions for one unit cell. In (a) we observe at each value of E_i three diffraction peaks, associated to the zero (specular) and first diffraction orders. They appear at Bragg angles of 0° and ±15.7° for $E_i = 21$ meV, and 0° and ±9.2° for 63 meV, respectively. Since in the CD functions of the inset the rainbow angles (extrema) appear at ±12.2° and ±9.2°, we conclude that the first-order peaks at $E_i = 63$ meV display a quantum rainbow feature, and the whole diffraction pattern is associated to the surface rainbow. This fact has also the effect of decreasing the specular integrated intensity (area under the diffraction peak) and

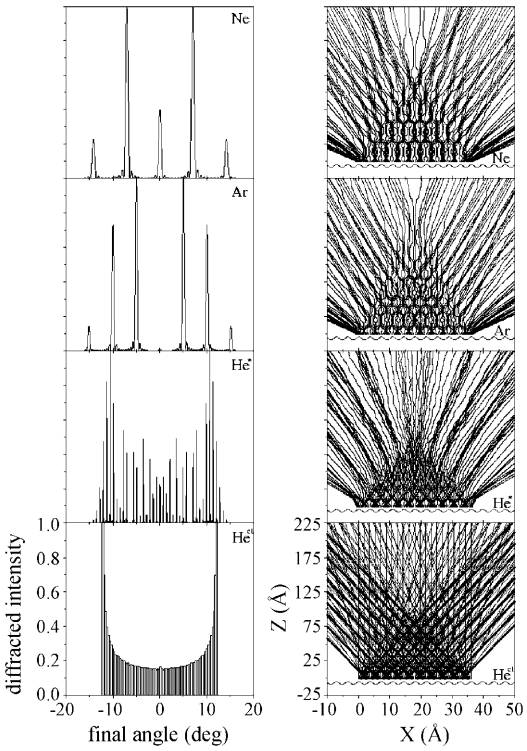

Fig. 2 – Intensity diffraction pattern (a) and quantum trajectories (b) at 21 meV and normal incidence for the Ne, Ar, He^*, and He^{cl}-Cu(110) scattering. To make the comparison easier, the intensities have been normalized to their maximum values.

increasing those of the first-order peaks with respect to the scattering at 21 meV. In the semi-classical picture, trajectories contributing to the peaks located at $\pm 15.7°$, which do not fulfill the quantum rainbow condition, are classically forbidden but energetically allowed. Therefore, only complex valued classical trajectories are responsible for such weak-intensity peaks [19].

In the BB formalism it is not necessary to resort to such complex trajectories to describe the classically forbidden dynamics, and the QD function plotted in fig. 1(b) is readily interpreted in terms of Bohmian trajectories. This function presents a ladder-type shape linked to the Bragg angles, in sharp contrast with the smooth character of the CD function. As demonstrated in [9], the length of each step corresponds to a specific portion of the incident wave packet, which is responsible for each diffraction channel. In this way, the center of the packet is associated to the specular peak (central step), and small portions at the borders are the origin of the first- and higher-order peaks (remaining steps in the QD function). Furthermore, the density of trajectories in each one of these steps, weighted with the probability derived from the initial wave packet, is proportional to the corresponding diffraction intensity. Obviously, the finite spatial width of the wave packet manifests itself in the border effect, present in the QD function. Notice also that all information relevant for the classical dynamics is restricted to only one unit cell, whereas in quantum treatments the whole region illuminated by the initial wave packet is involved in the dynamics.

In fig. 2 the results corresponding to the diffraction intensities (left column) and their associated Bohmian trajectories (right column) at $E_i = 21$ meV for incoming particles of

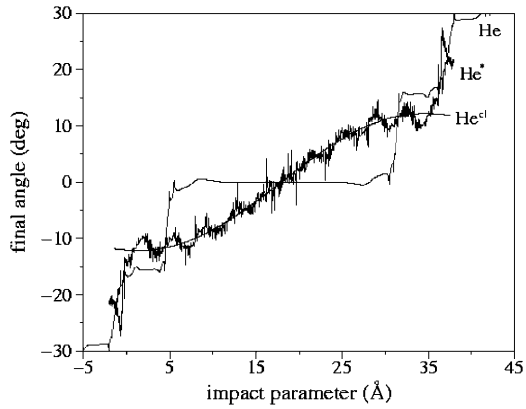

Fig. 3 – Quantum deflection function at 21 meV and normal incidence for He and He*-Cu(110) scattering, and classical deflection function normalized to the width of the initial wave packet.

different masses (Ne, Ar, and He*) are depicted. The trajectories are only plotted in the region near the surface (analogous to the Fresnel region of undulatory optics [9]), and to avoid complicating the figure we have not represented their incident parts, where, due to the lack of interaction, nothing interesting happens. For comparison, the classical results for He (labelled He^{cl}) are also shown at the bottom of the figure.

In the left column it is clearly seen that the number of diffraction peaks increases with the mass of the scattered particles, approaching the limit of the classical distribution (bottom). At the same time, the specular peak gradually disappears (consider also fig. 1(a) as the first member in the series of results) and an oscillatory behavior in the intensity peaks appear (see results for He*). Regarding the right column, several comments are in order. First, the topology of the trajectories becomes more and more complex as m increases; the trajectories get more wiggly with numerous crossings and anticrossings among them. This can be explained by invoking the hydrodynamical interpretation of quantum mechanics [8], in which light particles move within a laminar flux, whereas as m increases a transition to a turbulent regime takes place. Second, and more important, the displayed patterns evolve, in the limit of very high masses, towards the classical results, as can be ascertained by comparing the results of He* and He^{cl}. However, there exists a substantial difference between them. In the classical case, the CD function is periodic, covering densely the interval between the two rainbow angles, where the caustics appear. On the contrary, Bohmian trajectories for He* are bunched in groups pointing in the direction of the different Bragg angles and, in particular, of rainbow angles. The rainbow formation mechanism in both cases is quite different; while in the former one rainbow is originated at each unit cell, in the latter the accumulations are caused by the trajectories at the borders of the illuminated surface area. This is a direct consequence of the non-local character of Q, which is important even for these high values of m. For the same reason, the diffracted intensity in the left column shows strong oscillations as opposed to the smooth profile corresponding to the classical case (bottom). Let us remark that these accumulations, when completely defined in the Fraunhofer region [9], give rise to each of the diffraction peaks observed. And third, it should be noticed that simultaneously the quantum trajectory pattern near the surface becomes very similar to that of the classical one.

In fact, the previous discussion deals with the problem of how the classical limit emerges from quantum mechanics according to the correspondence principle, which constitutes the

main objective of this letter. To further analyze this result, we show in fig. 3 the QD function for He and He* at the scattering conditions considered above. By comparing these two curves, the transition from a discrete, ladder-shape behavior, typical of the quantum regime, to a more continuous dependence, characteristic of classical studies, with the impact parameter is readily apparent. More importantly, the average of the QD function for He* is in excellent quantitative agreement with the CD function for He$^{\rm cl}$ (plotted in the inset of fig. 1) when normalized in width to the number of units cells (ten in our case) spanned by the initial wave packet. Such a result unambiguously confirms the clear influence of the classical regime in the process that we are considering, the whole diffraction pattern being determined by the rainbow condition, although the non-local character of the quantum dynamics is preserved. This is an illustration of the great performance of the BB theory, which is more demanding computationally, but provides a better intuitive insight. In some sense, the fact that the diffraction intensities for He* and He$^{\rm cl}$ in fig. 2 present a similar pattern is also a reflection of this result; the difference being that in the first case we have a probabilistic interpretation while in the second the interpretation is causal, as in classical mechanics.

A final point worth mentioning is the existence of modulations in the QD function of fig. 3, which displays a clear ten-period oscillation derived from how the surface corrugation is "seen" by the initial wave packet. There also exist faster (smaller) fluctuations as a direct consequence of the quantum potential, Q, which goes to zero as m increases.

Summarizing, in this letter the classical limit in atom-surface scattering has been studied from the causal point of view provided by the BB theory. By using Bohmian trajectories, we have been able to unveil the mechanism by which the quantum rainbow appears, and show that the differences between the quantum diffraction pattern and the classical results tend to disappear when $Q \to 0$, despite the fact that the global character of the dynamics is not achieved in this limit. The corresponding distribution of Bohmian trajectories mimics that of the classical study, presenting accumulations at the rainbow angles, although the origin of these two effects is completely different. We think that this type of studies constitutes a very powerful and intuitive tool for the description of quantum phenomena.

* * *

This work has been supported in part by DGES (Spain) under contracts No. PB95-71, PB96-76, PB98-115 and BFM2000-347. ASS gratefully acknowledges a doctoral grant from the Consejería de Educación y Cultura of the Comunidad Autónoma de Madrid (Spain).

REFERENCES

[1] Farías D. and Rieder K. H., *Rep. Prog. Phys.*, **61** (1998) 1575.
[2] Grisenti R. E., Schöllkopf W., Toennies J. P., Hegerfeldt G. C. and Köhler T., *Phys. Rev. Lett.*, **83** (1999) 1755.
[3] Doak R. B., Grisenti R. E., Rehbein S., Schmal G., Toennies J. P. and Wöll C., *Phys. Rev. Lett.*, **83** (1999) 4229.
[4] Ballentine L. E., *Phys. Lett. A*, **261** (1999) 145.
[5] Schöllkopf W. and Toennies J. P., *Science*, **266** (1994) 1345; Arndt M., Nairz O., Vos-Andreae J., Keller C., van der Zouw G. and Zeilinger A., *Nature*, **401** (1999) 680.
[6] Bohm D., *Phys. Rev.*, **85** (1952) 166; 194.
[7] Bohm D. and Hiley B. J., *The Undivided Universe* (Routledge, New York) 1993; Holland P. R., *The Quantum Theory of Motion* (Cambridge University Press, Cambridge) 1993.
[8] Lopreore C. L. and Wyatt R. E., *Phys. Rev. Lett.*, **82** (1999) 5190.

[9] Sanz A. S., Borondo F. and Miret-Artés S., *Phys. Rev. B*, **61** (2000) 7743.
[10] Philippidis C., Dewdney C. and Hiley B. J., *Nuovo Cimento B*, **52** (1979) 15; Dewdney C. and Hiley B. J., *Found. Phys.*, **12** (1982) 27; Dewdney C., Holland P. R., Kyprianidis A. and Vigier J. P., *Nature*, **336** (1988) 536; Dey B. K., Askar A. and Rabitz H., *J. Chem. Phys.*, **109** (1999) 8770; Wyatt R. E., *J. Chem. Phys.*, **111** (1999) 4406; Gindensperger E., Meier C. and Beswick J. A., *J. Chem. Phys.*, **113** (2000) 9369.
[11] Goldstein H., *Classical Mechanics* (Addison-Wesley, Reading, Mass.) 1980.
[12] Gorse D., Salanon B., Fabre F., Kara A., Perreau J., Armand G. and Lapujoulade J., *Surf. Sci.*, **147** (1984) 611; Miret-Artés S., Toennies J. P. and Witte G., *Phys. Rev. B*, **54** (1998) 5881.
[13] Rieder K. H. and Stocker W., *Phys. Rev. B*, **31** (1985) 3392.
[14] Hernández M., Miret-Artés S., Villarreal P. and Delgado-Barrio G., *Surf. Sci.*, **274** (1992) 21; Hernández M., Miret-Artés S., Villarreal P. and Delgado-Barrio G., *Surf. Sci.*, **339** (1995) 205.
[15] Miret-Artés S., Margalef-Roig J., Guantes R., Borondo F. and Jaffé C., *Phys. Rev. B*, **54** (1996) 10397; Guantes R., Borondo F., Jaffé C. and Miret-Artés S., *Surf. Sci.*, **338** (1995) L863.
[16] Borondo F., Jaffé C. and Miret-Artés S., *Surf. Sci.*, **317** (1994) 211.
[17] Berry M. V., *J. Phys. A*, **8** (1975) 566.
[18] Heller E. J., *J. Chem. Phys.*, **62** (1975) 1544; Drolshagen G. and Heller E. J., *J. Chem. Phys.*, **79** (1983) 2072.
[19] Guantes R., Borondo F., Jaffé C. and Miret-Artés S., *Phys. Rev. B*, **53** (1996) 14117.